Physica A 623 (2023) 128836

Contents lists available at ScienceDirect

Physica A

journal homepage: www.elsevier.com/locate/physa

An advanced control strategy for connected autonomous vehicles based on Micro simulation models at multiple intersections

Jie Wang [a], Zhiyu Cai [c], Yaohui Chen [a,b], Peng Yang [a], Bokui Chen [a,b,*]

[a] *Tsinghua Shenzhen International Graduate School, Tsinghua University, China*
[b] *Peng Cheng Laboratory, Shenzhen, China*
[c] *Department of Civil and Environmental Engineering, University of California, Berkeley, CA 94720, USA*

ARTICLE INFO

Article history:
Received 1 February 2023
Received in revised form 18 April 2023
Available online 9 May 2023

Keywords:
Connected automated vehicles
Intersection
Cellular automaton
Conflict
Downstream density

ABSTRACT

The high controllability and connectivity of connected automated vehicles (CAVs) have created opportunities to enhance the road network's performance. Considering the case that all vehicles in the road network are CAVs, we build an intersection model in which all CAVs follow a given route through the intersection. We obtain the basic evolution rules of vehicles based on the cellular automata model and design conflict judgment and speed adjustment rules to ensure the passage of CAVs within intersections without conflicts. Further, with the goal of minimizing traffic delays in the road network, we design a coordinated control strategy for multiple intersections by considering the density of downstream vehicles. Finally, we conduct simulation experiments in different traffic scenarios. The results show that as the vehicle arrival rates rise, CAVs' average delays rise and their average speeds decrease. The growth rate of traffic flow through the intersection slows down when a certain percentage is reached. Meanwhile, the coordinated control strategy for multiple intersections can obtain a minor average delay of vehicles on the road network.

1. Introduction

Intelligent transportation system [1] is an important technology that has gradually become a breakthrough in resolving traffic problems. It alleviates traffic congestion, improves traffic safety, and reduces traffic contamination. Connected autonomous vehicles (CAVs) can obtain information about the speed and location of surrounding vehicles via vehicle-to-vehicle communication, considering the effect of them on target vehicle following and lane-changing behavior. This can effectively predict the future driving behavior of surrounding vehicles and respond promptly to enhance the stability of traffic flow and improve road capacity [2–4]. The National Highway Traffic Safety Administration (NHTSA) believes that the annual death toll caused by road traffic accidents will decrease by about 17,000 each year as the proportion of connected vehicles rises and the death toll from road traffic accidents is expected to be reduced to the current 50% by 2050 [5].

The intersection is an important part of the urban road. The efficiency of vehicles at the intersection significantly impacts the overall operational efficiency of urban traffic, and it is also the frequent site of traffic accidents [6]. Scholars are increasingly examining vehicle–vehicle communication and vehicle–road coordination, proposing different control

* Corresponding author at: Tsinghua Shenzhen International Graduate School, Tsinghua University, China.
E-mail address: chenbk@tsinghua.edu.cn (B. Chen).

https://doi.org/10.1016/j.physa.2023.128836
0378-4371/

strategies to improve the safety of intersections and increase traffic flow. Related research can be classified into two categories: "signal optimization" and "vehicle guidance". "Signal optimization" researches focus on optimizing the signal cycle, green light duration, and phase of the intersection based on information such as vehicle speed and location [7–9]. Whereas intersection control optimization strategies based on vehicle guidance are primarily concerned with planning the optimal path and speed for vehicles to achieve efficient and safe passage of vehicles at intersections [10–13]. Different methods of observing traffic behavior exist, including microscopic, mesoscopic and macroscopic simulation models [14]. Due to the complexity and variability of traffic flow characteristics, it is necessary to treat traffic as individual driver–vehicle objects at the micro level and study the traffic flow characteristics at intersections in the networked environment to verify the effectiveness of this method.

Cellular automata [15,16] were first proposed by Von Neumann in the 1950s and are mainly used to simulate the self-replication function of living systems. Due to the discrete-time, space, and state variables of the cell, the cell state is updated locally in parallel, making it suited for computer implementation and enabling quick calculation of extensive road networks. Since then, many researchers have improved the cellular automata model based on different regulations in order to simulate a more realistic traffic environment and more precisely reflect the characteristics of traffic flow [17–21], which is also applied in the field of intersection [22,23]. With the emergence of CAVs, cellular automata models are also used to simulate their operation at intersections. Zhao et al. [24] analyzed the impact of CAV penetration rate on passing speed and delay time at a signalized intersection. Jiang et al. [25] combined the cellular automata model and the ant colony model to explore the single intersection's mixed traffic flow.

CAVs are likely to become the mainstay of urban roads in the future, by which time all vehicles will share their driving information in real-time, making traffic lights unnecessary [26]. In the absence of signal control, Luis et al. [27] combines genetic algorithms with cellular automata to improve the performance of intersections by optimizing vehicle arrival rates. Wu [28] established a cellular automaton model to stimulate the operation of traffic flow in the intersection using a greedy algorithm so that the conflicting networked vehicle queues can safely pass through the intersection through cooperation. However, when a vehicle queue in one direction is permitted to pass, all vehicles in other directions need to wait. This model is controlled in units of each vehicle queue like an invisible signal light. However, when a vehicle queue in one direction is permitted to pass, all vehicles in other directions need to wait, which are controlled in units of each vehicle queue like an invisible signal light.

In our study, we treat each car as the smallest control unit. Considering that all vehicles on the road are CAVs, we build a fully controlled intersection model where vehicles' routes are determined. By formulating the control strategy based on the cellular automata model, under the premise of ensuring safety, CAVs in all entrance lanes in each direction can pass without waiting for the entire platoon of vehicles, which minimizes vehicle delay and queue length at the intersection. Then, on this basis, we propose a multi-intersection control strategy that takes into account the vehicle density in various segments of the road network. Finally, the vehicles' running efficiency at intersections under the two control strategies is compared by numerical simulation.

The remaining sections of the paper are organized as follows. Section 2 establishes an intersection scene where vehicles have fixed routes. Section 3 proposes a single-intersection control strategy and a regional multi-intersection coordinated control strategy for CAVs. In Section 4, we conduct simulation experiments to investigate the effects of the two control strategies under different traffic flow distributions. Finally, our summary is in Section 5.

2. Intersection scenario setup

We establish a two-way eight-lane intersection, similar to the scenario set by Rhythm Control [10] of automatic traffic. Setting that CAVs on each lane will pass through the intersection according to the established and reasonable route to reduce the conflicts of vehicles on different lanes at the intersection. The entrance lanes in all directions have one right turning lane, two straight lanes, and one left turning lane. CAVs in right turning lane do not conflict with vehicles in any other lanes, while left turning lane and straight lanes have possible conflict points with six different lanes, as shown in Fig. 1. As a result, the area where CAVs will collide is only the space of 6×6 cells in the center, which is regarded as an intersection conflict area, for the right turn lane will not be disturbed.

At the same time, it is assumed that vehicles will pass through a certain length of non-adjusted area before entering the intersection, where CAVs cannot change lanes or overtake vehicles in this area. On the one hand, chaos and conflicts at the intersection are reduced and driving safety is ensured. On the other hand, when a vehicle enter the area, they are considered to have entered a designated route based on their destination, and the intersection control center will begin to determine if the vehicle conflicts with another vehicle. Therefore, CAVs need to select the appropriate left-turn, straight-turn, or right-turn lane according to their respective driving destinations before entering the vicinity of the intersection. CAVs are free to drive in other areas except for inside intersections and non-adjusted zones. It is known which lanes the CAVs may conflict with other vehicles because the route of the particular vehicle is known and determined. They are referred to as the conflicting lane, forming a conflicting lane set in order of precedence. Therefore, for each CAV i, except for right-turning ones, there are several predetermined locations on its travel route within the intersection that will overlap with the travel routes of vehicles in its conflicting lane set, called conflict points.

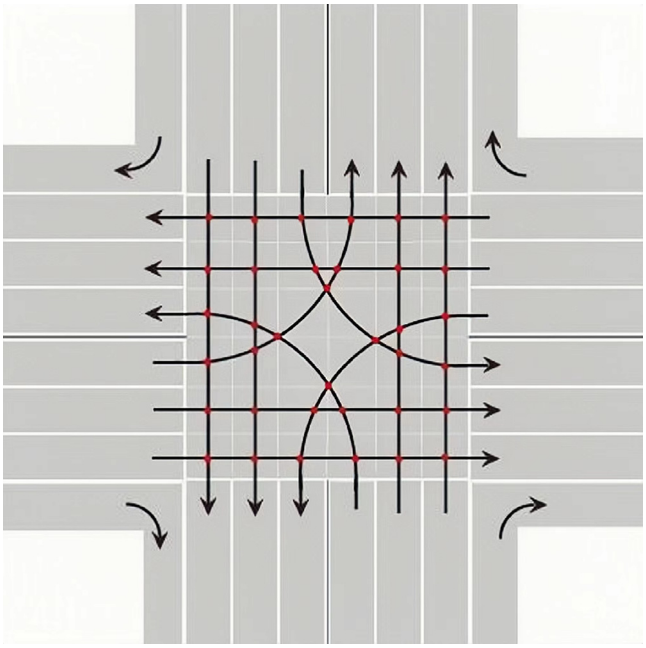

Fig. 1. Illustration of the intersection.

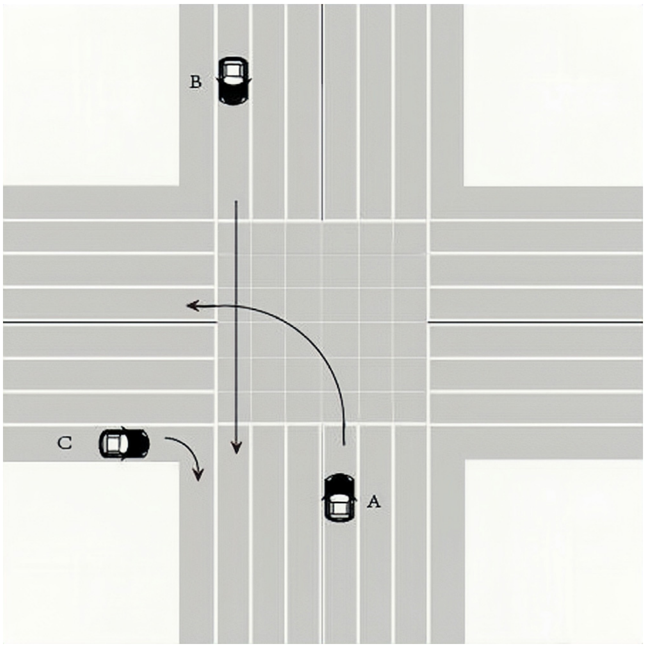

Fig. 2. Illustration of CAVs' driving route.

Example 1:

The intersection example is shown in Fig. 2. CAV A is in the left turn lane of the southern entrance path, CAV B is in the straight lane of the west entrance road, and CAV C is in the north entrance road's right turning lane. Inside the intersection, there are five conflict points on the driving path of CAV A, which will conflict with lanes in six directions. CAV B has six conflict points for incoming vehicles from six directions, while CAV C has no conflict points.

3. Micro simulation models for intersection traffic flow

In this section, a single-intersection control strategy (SICS) is proposed based on the cellular automata model and, based on this, a regional multi-intersection control strategy (MICS) with coordinated control.

3.1. Micro simulation models for traffic flow at single intersection

We simulate the behavior of CAVs in the real world using the cellular automata model. The operation of vehicles at intersections can be divided into two parts: basic evolution rules and conflict judgment and speed adjustment. Among them, we refer to the classical MCD model [29] to design the basic evolution rules of CAVs on the road.

3.1.1. Basic evolution rules

- Speed Up:
  CAVs increase the speed with a certain acceleration to ensure traffic efficiency without exceeding the maximum speed:

$$v_i(t+1) = min(v_{max}, v_i(t)+1) \tag{1}$$

  where $v_i(t)$ is the CAV i's speed of at time t, and v_{max} is the preset maximum speed of vehicle.

- Speed Update:
  CAVs reduce their pace stochastically, with a certain probability, in order to simulate driving conditions on actual roads:

$$v_i(t+1) = \begin{cases} max(0, v_i(t+1)-1) & p \leq p_0 \\ v_i(t+1) & p > p_0 \end{cases}, \tag{2}$$

  where p_0 is the probability of random speed reduction, and p is a randomly generated number between 0 and 1.

- Speed Reduction depending on the condition of the CAV ahead:
  In the process of driving, it is vital to modify the vehicle's speed and maintain an appropriate distance from the vehicle ahead based on their position and speed in order to ensure safety:

$$v_i(t+1) = min(v_i(t+1), v_{i+1}(t+1) + d_i - 1), \tag{3}$$

  where d_i represents the number of vacant cells between the CAV i and the vehicle that preceded it, that is, the distance between the two vehicles, which is shown in Fig. 3.

- Location Update: The position of CAV i at moment $t+1$ is:

$$x_i(t+1) = v_i(t+1) + x_i(t), \tag{4}$$

  where $x_i(t)$ is the CAV i's position at time t.

3.1.2. Conflict judgment and speed adjustment criteria

In the intersection area, the intersection controller collects information on the surrounding CAVs through V2I [30] and ensures the safe and efficient passage of vehicles based on the basic vehicle evolution rules and conflict judgment and speed adjustment criteria. The SICS is shown in Fig. 4.

First, for the CAV i whose travel trajectory is inside the intersection at the moment $t+1$, we obtain $v_i(t+1)$ according to Eq. (1)–Eq. (3). Second, the intersection controller needs to judge whether the driving trajectory of CAV i will collide with other vehicles in its conflicting lane set. If there is a CAV in its conflicting lane set also passes the conflict point at the moment of $t+1$, it means that a conflict will occur. We set

$$conflict = \begin{cases} 1 & x_j(t) < H, x_j(t) + v_j(t+1) \geq H \\ 0 & otherwise \end{cases}, \tag{5}$$

where CAV j is on the conflicting lane K_b of CAV i, H represents the location of the conflicting point between CAV i and CAV j on lane K_b and *conflict* is an indication of whether or not a conflict will occur.

If *conflict* $= 1$, then the right-of-way is assigned according to the "first come first to occupy" rule, and the CAV i's speed is updated based on the following equation:

$$v_i(t+1) = \begin{cases} v_i(t+1) - D_i - 1 & D_i/v_i(t+1) > D_j/v_j(t+1) \\ V_i(t+1) & D_i/v_i(t+1) < D_j/v_j(t+1) \end{cases}, \tag{6}$$

where D_j and D_i respectively represent the distance between CAV j and CAV i and the conflicting point. If CAV i arrives at the conflict point later, it needs to decelerate and maintain a feasible maximum speed to ensure efficiency while not

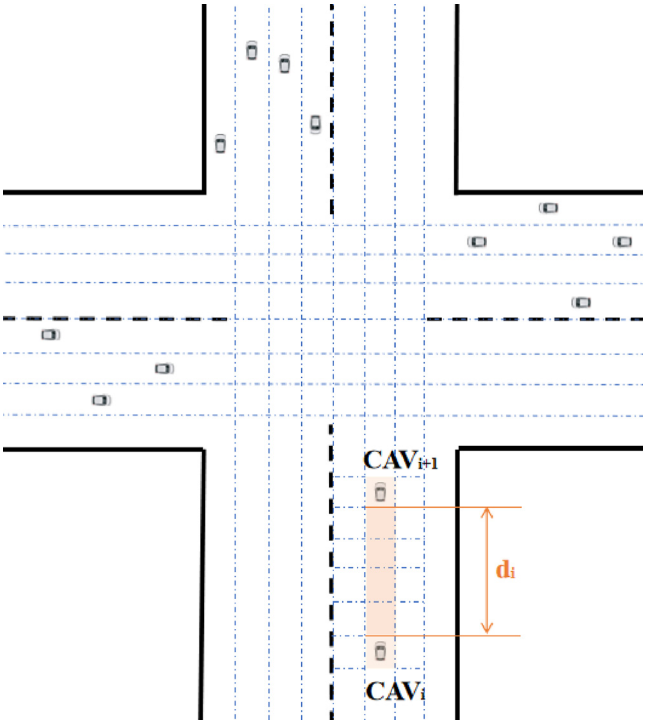

Fig. 3. Illustration of the distance between CAVs.

reaching the point of conflict [24]. On the contrary, no adjustment is required if it arrives at the conflict point earlier. Coincidentally, suppose CAV i arrives at the conflict point simultaneously as CAV j. In this case, if the conflict is between a left-turn vehicle and a straight-through vehicle, the straight-through vehicle will be accorded the road right priority; if the conflict is between two straight-through vehicles or two left-turn vehicles, the road right will be given randomly. Finally, the position of CAV i at moment $t + 1$ is updated according to Eq. (4).

3.2. Micro simulation models for traffic flows at multiple intersections

Intersection is the basic component unit of the road network. The vehicle traffic control of a single intersection is the basis for the linkage of urban arterial roads and the coordinated control of intersection groups. However, as the scale of the urban transportation system expands and the quantities of CAVs in the transportation network increases, the intersections become increasingly close. The optimal vehicle dispatching strategy for a single intersection only considers how efficiently vehicles can pass through the target intersection without considering the traffic flow of surrounding intersections. It is only a local optimum, not a system optimum, for the urban traffic system [31].

In urban road networks, the distribution of residential areas, commercial centers, etc., is usually concentrated, which inevitably leads to different traffic attractiveness of different locations at different times of the day [32]. As a result, the traffic flows in different sections or directions in the road network are also different. The function of an intersection is not only to ensure efficient, safe, and orderly movement of vehicles at that point but also to consider its impact on the operational efficiency of the road network traffic.

As shown in Fig. 5, CAV A arrives at the south import road, and CAV B arrives at the west import road of the intersection. The traffic densities downstream of their exit lanes are different. In this case, the control strategy of the intersection should make adaptive adjustments to avoid further blockage of the aggravated congestion section as much as possible to optimize the traffic operation efficiency of the road network.

However, using a centralized controller to control all vehicles in the road network is impractical. As the quantities of vehicles in the transportation network increases, centralized controllers cannot avoid dimensional disasters [33]. Therefore, each intersection is still considered to correspond to a controller in multi-intersection coordination control. The controller assigns the right-of-way to the vehicles passing through that intersection. At the same time, adjacent intersections can communicate to obtain the vehicle density information of downstream roads. The vehicle traffic rules of each controller will consider not only the inflow of vehicles in different directions and lanes of that intersection but also the vehicle density of the downstream road to adjust its control strategy and transmit the information to the surrounding vehicles.

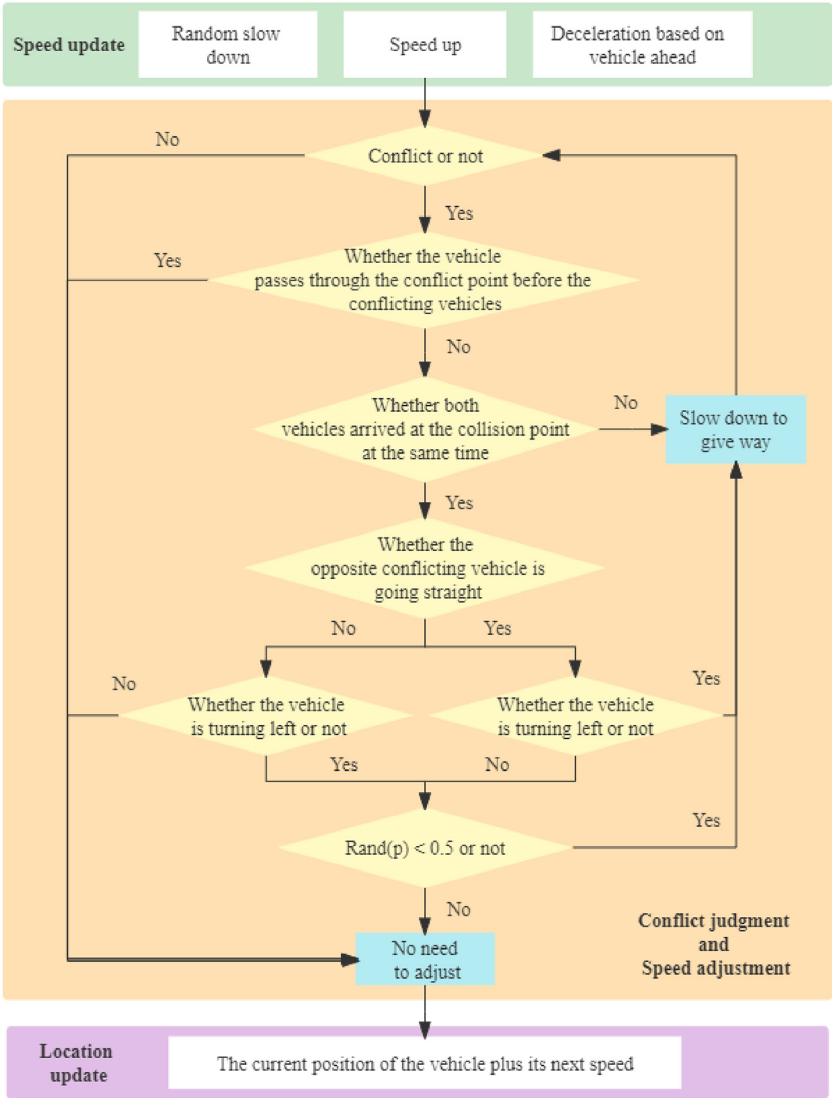

Fig. 4. Single-intersection control strategy.

The following two considerations will be added to the MICS compared to SICS.

3.2.1. Maximum speed limit

Traffic flow, traffic density, and average velocity are typical parameters utilized to characterize traffic flow. In 1996, the GreenShield model [34] proposed a linear speed–density relationship:

$$\bar{V}_s = V_f(1 - \frac{K}{K_j}), \tag{7}$$

where V_f represents the velocity of free flow and K_j represents the blockage density.

When the road vehicle density increases, the average vehicle speed decreases. Although the GreenShield model can reveal the relationship between road density and vehicle speed relatively accurately, it is not accurate enough when the road vehicle density is too low [35]. Considering that most urban roads have certain speed limit policies, Du et al. [36] modifies the model so that as the density is below the free-flow density threshold p_f, vehicles are allowed to keep traveling at free-flow speed. When p_f is exceeded, the speed will decrease linearly:

$$V = f_v(\rho) = \begin{cases} V_f & \rho \leq \rho_f \\ k_s(\rho - \rho_s) + V_f & \rho > \rho_f \end{cases} . \tag{8}$$

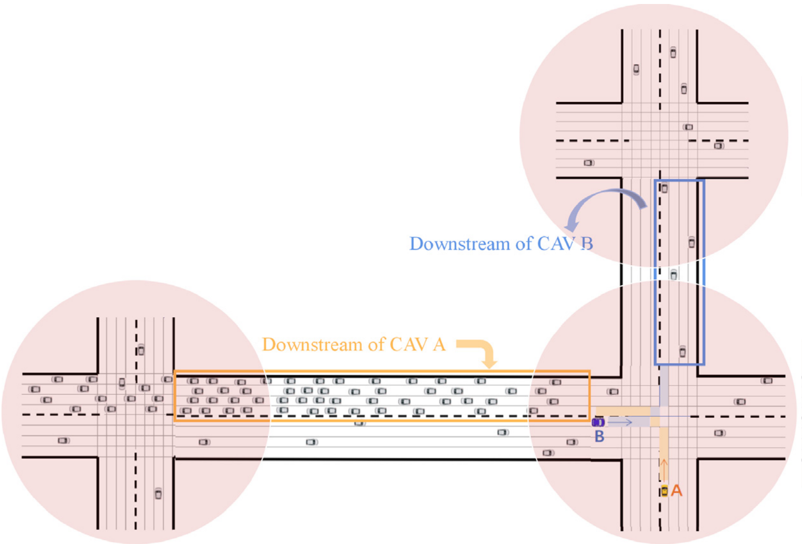

Fig. 5. Illustration of the intersection.

In our multi-intersection control strategy, neighboring intersections can share information about the vehicle density within their respective ranges. When an intersection judges that two vehicles will clash at a certain point, the intersection controller will adjust the speed of the CAV with higher density downstream according to the modified GreenShield model. Thus, a CAV with a higher density downstream may enter the intersection at a lower speed, while the control center may give the right of way to the opposing vehicle.

3.2.2. Allocation of vehicle rights-of-way for the road network

In the single intersection control strategy, when two CAVs arrive at the conflict point simultaneously and both are straight or left-turning vehicles, they will be randomly given the right-of-way in the single-intersection control strategy introduced in chapter 3.1. However, in the regional multi-intersection coordinated control strategy, the density situation of the vehicle downstream section needs to be considered. If a certain vehicle has a higher density downstream, joining the downstream convoy will increase traffic congestion. Therefore, if the collision occurs even after the maximum speed adjustment, in this case, the right-of-way should be given to the party with a lower downstream density, thus maximizing the traffic efficiency of the whole road network as much as possible. Based on the above rules, the intersection control strategy for regional multi-intersection coordination is shown in Fig. 6.

First, we update the speed of CAV i according to Eq. (1)–Eq. (3), and obtain *conflict* according to Eq. (5). If $conflict = 1$, judge the downstream density of CAV i and conflicting CAV j. When $\rho_{k_a} > \rho_{K_b}$, the downstream density is considered to calculate the maximum speed limit v'_{max} of CAV i:

$$v'_{max} = f_v(\rho_{k_a}) = \begin{cases} V_f & \rho_{k_a} \le \rho_f \\ k_s(\rho_{k_a} - \rho_s) + V_f & \rho_{k_a} > \rho_f \end{cases}, \tag{9}$$

where ρ_{k_a} and ρ_{K_b} represent the downstream vehicle density of lane k_a and lane K_b, respectively. At the same time, update $v_i(t+1)$ under the maximum speed limit:

$$v_i(t+1) = min(v'_{max}, v_i(t+1)). \tag{10}$$

After the speed is adjusted, determine if there will be a conflict again. If $conflict = 1$, allocate the priority rights-of-way based on downstream density. The speed of CAV i at moment $t+1$ is:

$$v_i(t+1) = \begin{cases} v_i(t+1) - D_i - 1 & \rho_{k_a} > \rho_{K_b} \\ v_i(t+1) & \rho_{k_a} < \rho_{K_b} \end{cases}. \tag{11}$$

The intersection controller obtains downstream density by communicating with the surrounding intersections and assigns priority to the one with a lower downstream density. If coincidentally, the downstream density of both CAVs is the same, let the one that arrives first pass the intersection according to the rule in Chapter 3.1.2

4. Numerical simulation and analysis

4.1. Single intersection

We carry out the vehicle micro-simulation in Matlab 2022 to investigate the CAVs' operation at single intersections. We construct a space of 60 × 60 cells. Assuming that the lane width is 3.5 m, each cell represents a 3.5 × 3.5 m space

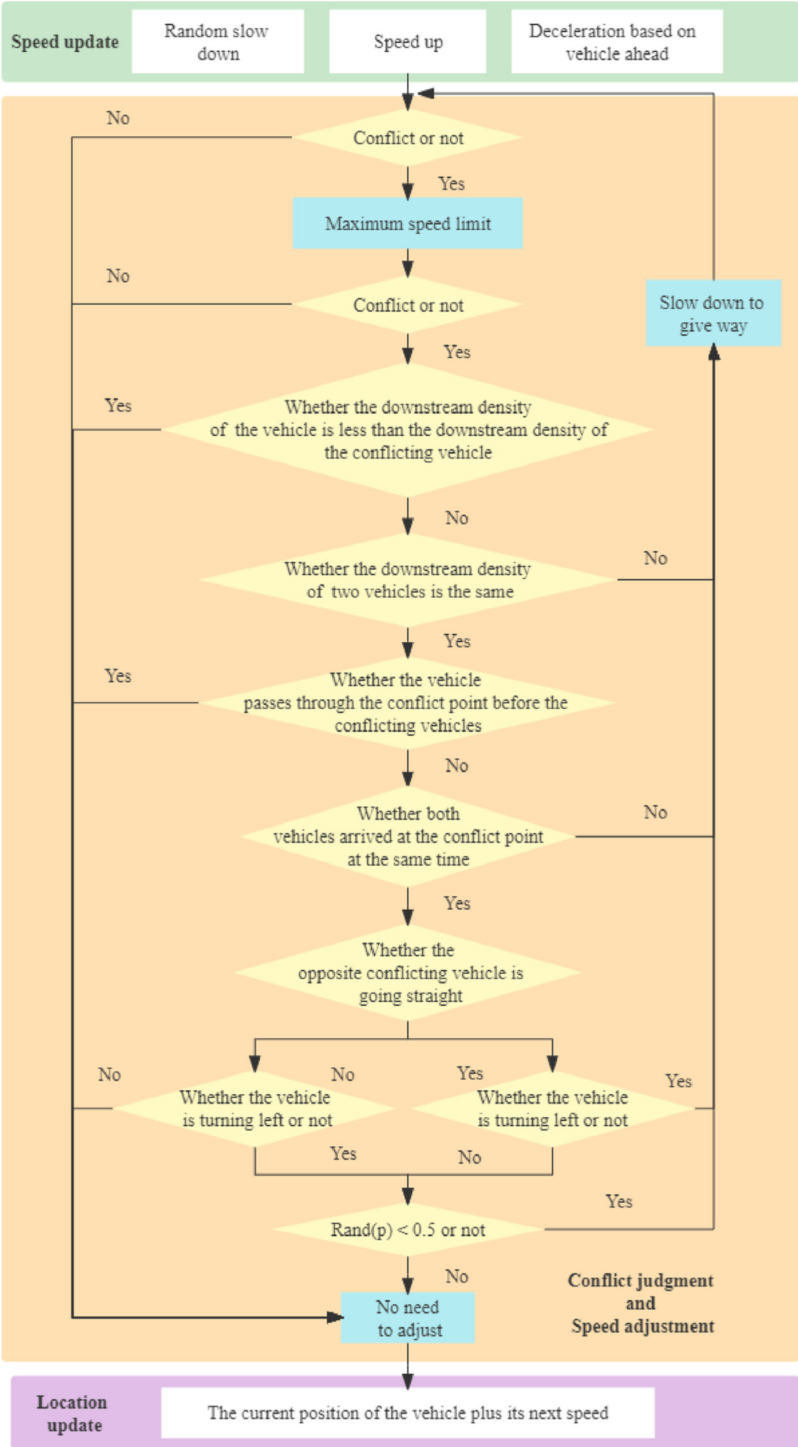

Fig. 6. Multi-intersection control strategy.

in the actual road scene, and the intersection conflict area is a 3 × 3 cell space. We use the open boundary simulation method [14] to simulate vehicle arrivals by generating new vehicles according to the set vehicle arrival coefficients without considering the end of the vehicle leaving the road. Since right-turning CAVs do not conflict with other vehicles, we only simulate the operation of left-turning and straight-through CAVs within the intersection. For the other simulation parameters, we set $vmax = 4cells/step$ (equals to 54 km/h), $p_0 = 0.1$, simulation step length $t = 1$ s and simulation

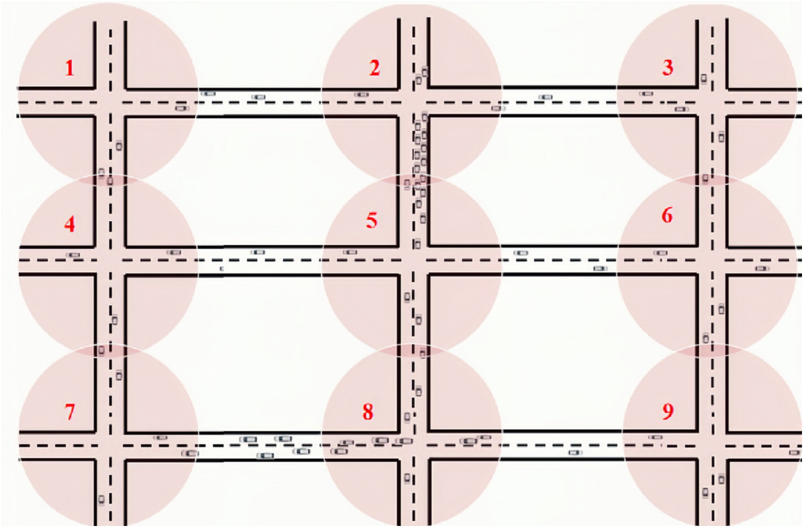

Fig. 7. Multi-intersection scenario.

cycle $T = 3600$ steps. In order to prevent the simulation results from being affected by random factors, we conduct 100 simulations and analyze the average of all the results.

We define that $\lambda = [\lambda_{S_l}, \lambda_{S_s}, \lambda_{W_l}, \lambda_{W_s}, \lambda_{N_l}, \lambda_{N_s}, \lambda_{E_l}, \lambda_{E_s}]$, corresponding to the arrival rate of vehicles in the left lane and straight lane at the entrance road in each of the four cardinal directions (south, west, north, and east). There two different scenarios to consider, i.e., balanced demand scenario (λ_1), imbalanced scenarios (λ_2, λ_3 and λ_4), their values are given below.

$$\lambda_1 = \left[1, 1, 1, 1, 1, 1, 1, 1\right] * \alpha$$

$$\lambda_2 = \left[0.8, 1.1, 0.8, 1.1, 0.8, 1.1, 0.8, 1.1\right] * \alpha$$

$$\lambda_3 = \left[0.6, 1.2, 0.6, 1.2, 0.6, 1.2, 0.6, 1.2\right] * \alpha$$

$$\lambda_4 = \left[0.4, 1.3, 0.4, 1.3, 0.4, 1.3, 0.4, 1.3\right] * \alpha$$

$$\lambda_5 = \left[1.2, 0.9, 1.2, 0.9, 1.2, 0.9, 1.2, 0.9\right] * \alpha$$

$$\lambda_6 = \left[1.4, 0.8, 1.4, 0.8, 1.4, 0.8, 1.4, 0.8\right] * \alpha$$

where the scaling factor α signifies the level of traffic demand [10].

With balanced demand, the straight lanes' vehicle arrival rate and that of left turning lanes are identical. With imbalanced demand in λ_2, λ_3 and λ_4, the straight lanes' vehicle arrival rate is higher than that of the left turning lanes. While in λ_5 and λ_6, the left turning lanes' vehicle arrival rate is higher than that of the straight lanes. Also, these parameters are set to ensure that the total quantities of CAVs entering the intersection are the same in all six cases, given that the intersection has one left turning and two straight lanes in each inlet direction.

4.2. Multiple intersections

For the multi-intersection scenario, we construct a region consisting of nine intersections, each of which is the same size as the intersection in the single intersection scenario, as shown in Fig. 7.

To simulate how vehicles operate in the actual world, all CAVs will change lanes randomly after passing through the intersection. The ratio of vehicles entering the intersection making a left turn, a straight shot, and a right turn is fixed at 1:2:1. We set four different traffic flow distribution cases as follows to investigate the optimization effect of the coordinated control strategy of multiple intersections on traffic efficiency under different road network traffic distribution.

$$L_1 = \begin{bmatrix} 0.4 & 0.4 & 0.4 & 0.4 & 0.4 & 0.4 & 0.4 & 0.4 & 0.4 \\ 0.4 & 0.4 & 0.4 & 0.4 & 0.4 & 0.4 & 0.4 & 0.4 & 0.4 \end{bmatrix}$$

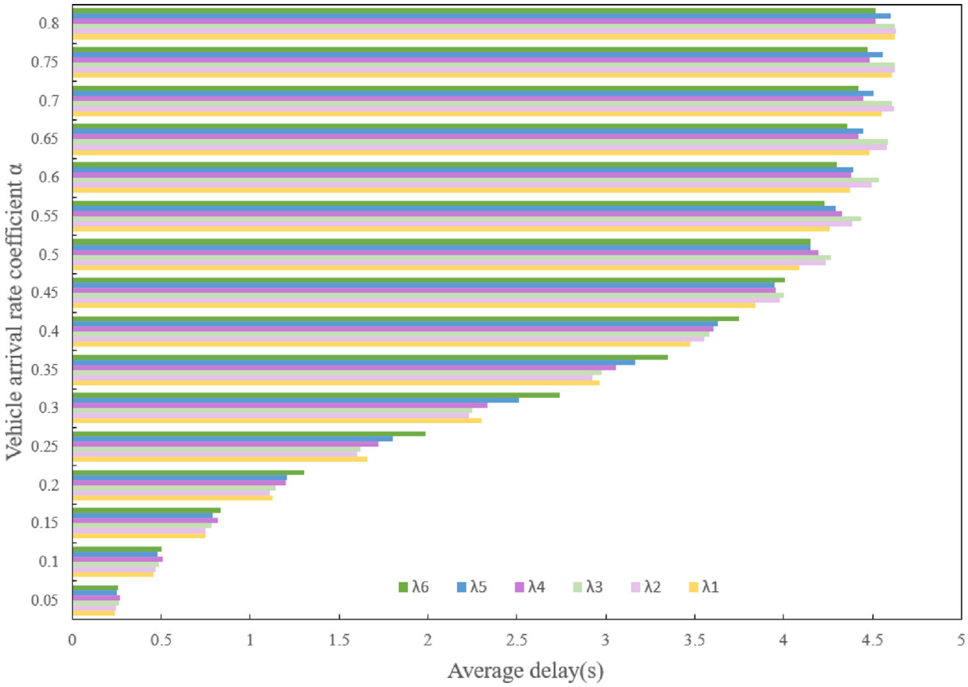

Fig. 8. Average delay of CAVs at intersection with vehicle arrival coefficient under four scenarios.

$$L_2 = \begin{bmatrix} 0.2 & 0.4 & 0.2 & 0.2 & 0.4 & 0.2 & 0.2 & 0.4 & 0.2 \\ 0.2 & 0.2 & 0.2 & 0.2 & 0.2 & 0.2 & 0.2 & 0.2 & 0.2 \end{bmatrix}$$

$$L_2 = \begin{bmatrix} 0.4 & 0.4 & 0.4 & 0.4 & 0.4 & 0.4 & 0.4 & 0.4 & 0.4 \\ 0.2 & 0.2 & 0.2 & 0.2 & 0.2 & 0.2 & 0.2 & 0.2 & 0.2 \end{bmatrix}$$

$$L_4 = \begin{bmatrix} 0.2 & 0.7 & 0.2 & 0.2 & 0.7 & 0.2 & 0.2 & 0.7 & 0.2 \\ 0.2 & 0.2 & 0.2 & 0.2 & 0.2 & 0.2 & 0.2 & 0.2 & 0.2 \end{bmatrix}$$

$$L_5 = \begin{bmatrix} 0.7 & 0.7 & 0.7 & 0.7 & 0.7 & 0.7 & 0.7 & 0.7 & 0.7 \\ 0.2 & 0.2 & 0.2 & 0.2 & 0.2 & 0.2 & 0.2 & 0.2 & 0.2 \end{bmatrix}$$

The first row and second row represent the traffic density distribution of the north–south and east–west entrance lanes at the nine intersections at the beginning of the simulation, respectively. Among them, L_1 indicates the case of balanced traffic demand on the road network, L_2 and L_4 denote a road network with a north–south road traffic flow greater than other road sections, while L_3 and L_5 represent a road network with both north and south lanes traffic flow greater than the east–west lanes.

We set the vehicle arrival rates in network for the five scenarios to 0.2, 0.4, and 0.6, respectively, and the simulation time $T = 3600$ s. The remaining parameters are kept consistent with the single-intersection scenario. To test the effectiveness of intersection control strategies after considering the maximum speed limit and downstream density-based intersection right-of-way assignment, we perform intersection simulations under two strategies, SICS and MICS, respectively, and compare their effects using the average vehicle delay at the intersection as the measure.

4.3. Simulation results and analysis

Figs. 8 and 9 depict the variation of the average delay and average speed of CAVs through the intersection with the vehicle arrival coefficient under six scenarios. Among them, CAVs' average delay at the intersection is obtained by subtracting the time at which vehicles passed through the crossing at the free flow speed from the actual time. It can be seen that when the vehicle arrival rate is small, CAVs are able to traverse the intersection smoothly with a relatively small delay. When the vehicle arrival coefficient is in the interval of 0.2 and 0.5, the average delay of vehicles increases significantly as the vehicle arrival rate rises because the quantities of CAVs on the road increases, the probability of conflict of CAVs inside the intersection increases, and therefore more CAVs need to slow down to give way. After the vehicle arrival coefficient is higher than 0.5, the growth in the average delay of vehicles inside the intersection slows down, eventually reaching about 4.5 s. Fig. 9 reveals that the average speed of CAVs within the intersection decreases as the vehicle arrival

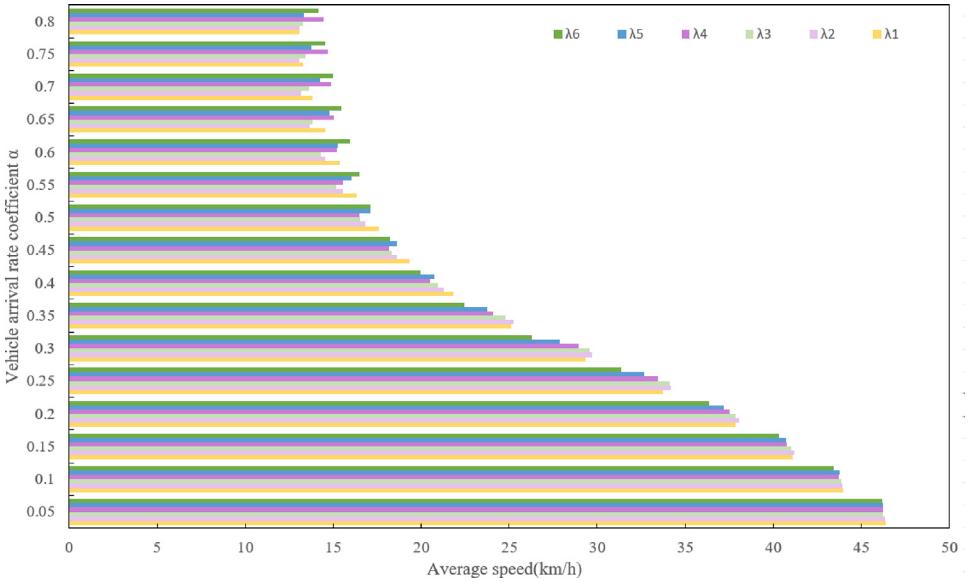

Fig. 9. Average speed of CAVs at intersection with vehicle arrival coefficient under four scenarios.

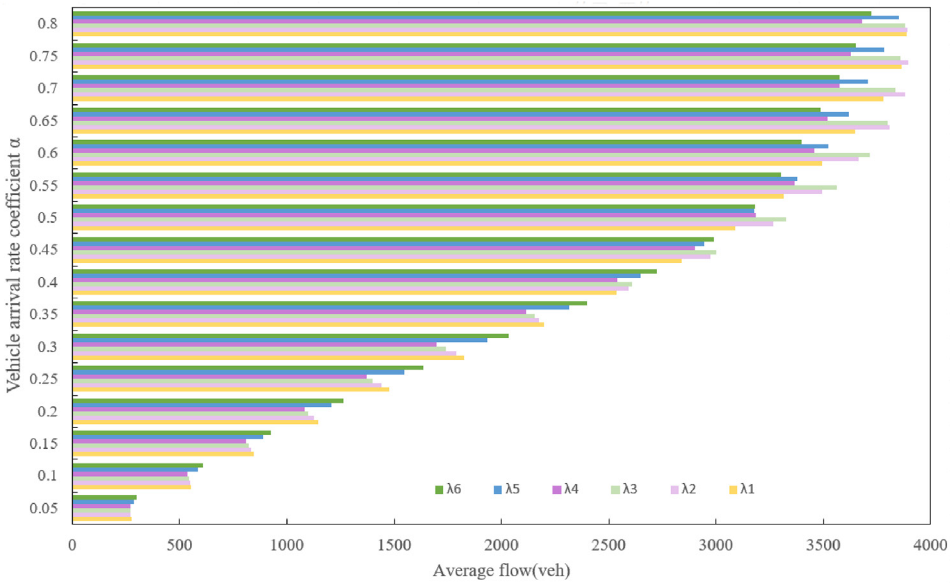

Fig. 10. Average flow through intersection with vehicle arrival coefficient under four scenarios.

rate increases, as vehicle deceleration and even stopping increases, which is consistent with the pattern in Fig. 8. When the vehicle arrival coefficient is higher than 0.5, the speed of CAVs within the intersection decreases more slowly. This is because the vehicles' speed is affected by the road vehicle density, and CAVs need to maintain a secure distance with the vehicle ahead to ensure safe driving. Fig. 10 manifests that the traffic flow in simulation time increases with the vehicle arrival rate in the four cases and gradually becomes saturated after the vehicle arrival coefficient is higher than 0.5.

Figs. 11–13 show the average vehicle delays of the road network based on SICS and MICS under different road network traffic distributions at a given vehicle arrival rate. It can be seen that MICS outperforms SICS for both balanced and unbalanced traffic distributions. The improved intersection coordination control strategy can reduce the average vehicle delay within the intersection for higher or lower vehicle arrival rates in the road network. To test the improvement effect of MICS on SICS, we set:

$$D_{Improve} = (D_{SICS} - D_{MICS})/D_{SICS} \tag{12}$$

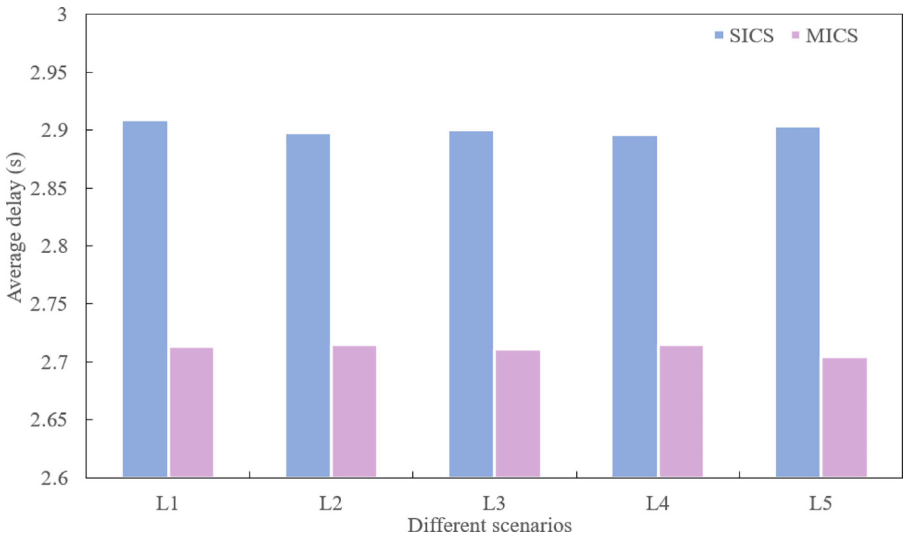

Fig. 11. Average delay at network intersections for different traffic distribution scenarios (Vehicle arrival rate = 0.2).

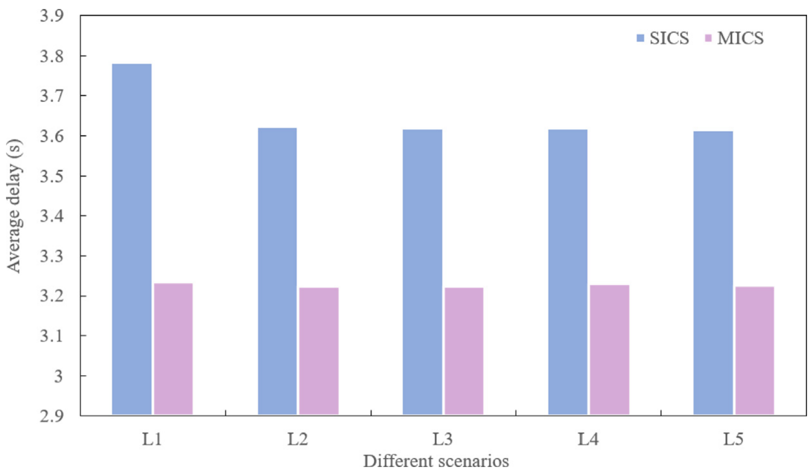

Fig. 12. Average delay at network intersections for different traffic distribution scenarios (Vehicle arrival rate = 0.4).

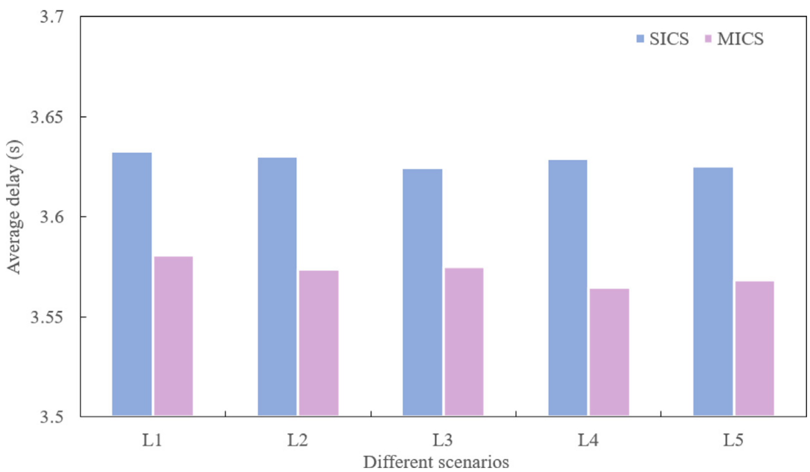

Fig. 13. Average delay at network intersections for different traffic distribution scenarios (Vehicle arrival rate = 0.6).

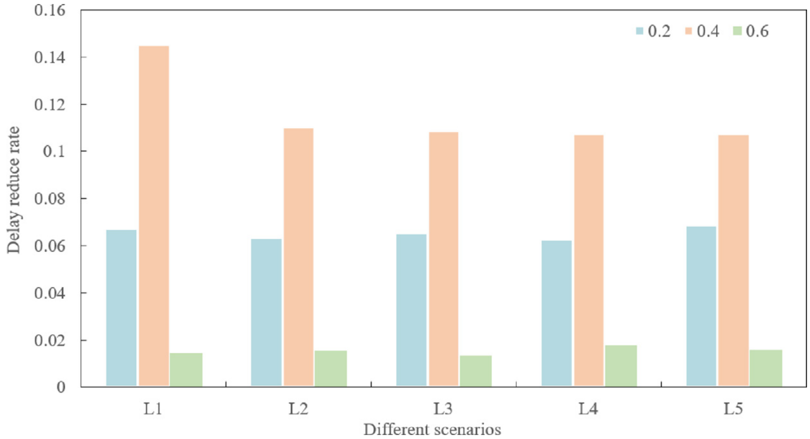

Fig. 14. The delay reduction rate of MICS for SICS under different vehicle arrival rates.

where $D_{Improve}$ is the delay reduction rate of MICS for SICS, D_{SICS} and D_{MICS} denote the delay of vehicles under SICS and MICS respectively.

The delay reduction rate of MICS to SICS is obtained for vehicle arrival rates of 0.2, 0.4, and 0.6. Fig. 14 reveals that the improvement rate of MICS to SICS is correlated with the transportation network's vehicle arrival rate. Under the five initial distribution scenarios of CAVs, when the arrival rate of CAVs on the road network is 0.4, the delay reduction rate of MICS is the highest compared with that of SICS, reaching 12% on average. When the arrival rate is 0.2, the delay reduction rate is about 7%. When the arrival rate is 0.6, the control effect is slightly improved. The experimental results manifest that the control strategy of incorporating downstream vehicle density into the intersection is effective.

5. Conclusions

In a fully networked environment where all road network vehicles are CAVs, we build an intersection model where CAVs follow a given route through the intersection, and the conflict points of vehicles inside the intersection are determined. Based on cellular automata model, we design a control strategy for a single intersection containing the basic evolution rules of CAVs and the conflict judgment and speed adjustment rules. Meanwhile, we add the maximum speed limit and the downstream density-based vehicle priority right-of-way assignment rules to the control strategy for multiple intersections from the perspective of minimum traffic delay in the road network. Based on these two strategies, we design different traffic flow distribution scenarios for numerical experiments. The results show that:

(1) As the rise of vehicle arrival rate, the likelihood of collisions within CAVs increases, leading to an increase in average delay inside the intersection and a decrease in the average vehicle speed.

(2) The volume of traffic through the intersection rises with the vehicle arrival rate. When vehicle arrival rate coefficient exceeds 0.5, CAVs need to maintain a certain safety distance from the CAV in front, resulting in a slower flow increase through the intersection.

(3) Under different initial distributions of traffic flow, the improved coordinated control strategy for multiple intersections can reduce the average delay of CAVs inside the road network intersections based on a given vehicle arrival rate.

In the future, more constraints and consideration of intersections of different sizes can be considered to simulate a more realistic road environment.

CRediT authorship contribution statement

Jie Wang: Conceptualization, Methodology, Software, Data curation, Writing – original draft, Writing – review & editing. **Zhiyu Cai:** Software, Validation, Data curation, Writing – original draft. **Yaohui Chen:** Investigation, Supervision, Project administration. **Peng Yang:** Software, Data curation. **Bokui Chen:** Conceptualization, Software, Formal analysis, Funding acquisition.

Declaration of competing interest

This manuscript has not been published and is not under consideration for publication elsewhere. All authors have approved the manuscript and agree with submission to Physica A: Statistical Mechanics and its Applications. We have no conflicts of interest to disclose. All figures are original obtained by us and any text taken from another paper is clearly indicated with the full source and permission of the authors of said source.

Data availability

The data that has been used is confidential.

Acknowledgments

This work was supported by the Project from Science and Technology Innovation Committee of Shenzhen (Grant No. JCYJ20210324115604012, JCYJ201908 (13173401651), Science and Technology Innovation Committee of Shenzhen-Platform and Carrier (International Science and Technology Information Center), the Tsinghua University Spring Breeze Fund (Grant No. 2021Z99CFW043), the Tsinghua-Toyota Joint Research Fund (Grant No. 20223930089), and the Tsinghua Shenzhen International Graduate School Fund (HW2020005, JC2021009, JC2022018).

References

[1] Y. Lin, P. Wang, M. Ma, Intelligent transportation system (ITS): Concept, challenge and opportunity, in: 2017 Ieee 3rd International Conference on Big Data Security on Cloud (Bigdatasecurity), Ieee International Conference on High Performance and Smart Computing (Hpsc), and Ieee International Conference on Intelligent Data and Security (Ids), IEEE, 2017., pp. 167–172.
[2] A. Talebpour, H.S. Mahmassani, S.H. Hamdar, Modeling lane-changing behavior in a connected environment: A game theory approach, Transp. Res. Procedia 7 (2015) 420–440.
[3] B. Chen, D. Sun, J. Zhou, W. Wong, Z. Ding, A future intelligent traffic system with mixed autonomous vehicles and human-driven vehicles, Inform. Sci. 529 (2020) 59–72.
[4] S. Yu, Z. Shi, The effects of vehicular gap changes with memory on traffic flow in cooperative adaptive cruise control strategy, Physica A: Stat. Mech. Appl. 428 (2015) 206–223.
[5] A. Demba, D.P. Möller, Vehicle-to-vehicle communication technology, in: 2018 IEEE International Conference on Electro/Information Technology, EIT, IEEE, 2018, pp. 459–464.
[6] I. Kotinas, A compilation of motor vehicle crash data from the fatality analysis reporting system and the general estimates system, Natl. Highw. Traff. Saf. Admin. 809 (2005) 775.
[7] Y. Feng, K.L. Head, S. Khoshmagham, M. Zamanipour, A real-time adaptive signal control in a connected vehicle environment, Transp. Res. C 55 (2015) 460–473.
[8] B.L. Smith, R. Venkatanarayana, H. Park, N. Goodall, J. Datesh, C. Skerrit, IntelliDriveSM Traffic Signal Control Algorithms, University of Virginia, 2010.
[9] Q. He, K.L. Head, J. Ding, Multi-modal traffic signal control with priority, signal actuation and coordination, Transp. Res. C 46 (2014) 65–82.
[10] X. Chen, M. Li, X. Lin, Y. Yin, F. He, Rhythmic control of automated traffic—Part I: Concept and properties at isolated intersections, Transp. Sci. 55 (5) (2021) 969–987.
[11] W. Sun, J. Zheng, H.X. Liu, A capacity maximization scheme for intersection management with automated vehicles, Transp. Res. Procedia 23 (2017) 121–136.
[12] L. Li, F. Wang, Cooperative driving at blind crossings using intervehicle communication, IEEE Trans. Veh. Technol. 55 (6) (2006) 1712–1724.
[13] J. Lee, B. Park, Development and evaluation of a cooperative vehicle intersection control algorithm under the connected vehicles environment, IEEE Trans. Intell. Transp. Syst. 13 (1) (2012) 81–90.
[14] M.K. Singh, K. Ramachandra Rao, Cellular automata models for signalised and unsignalised intersections with special attention to mixed traffic flow: A review, IET Intell. Transp. Syst. 14 (12) (2020) 1507–1516.
[15] S. Wolfram, Theory and Applications of Cellular Automata, World Scientific, 1986.
[16] T. Toffoli, N. Margolus, Cellular Automata Machines: A New Environment for Modeling, MIT Press, 1987.
[17] K. Nagel, M. Schreckenberg, A cellular automaton model for freeway traffic, J. Physique I 2 (12) (1992) 2221–2229.
[18] O. Biham, A.A. Middleton, D. Levine, Self-organization and a dynamical transition in traffic-flow models, Phys. Rev. A 46 (10) (1992) R6124.
[19] D.E. Wolf, Cellular automata for traffic simulations, Physica A: Stat. Mech. Appl. 263 (1–4) (1999) 438–451.
[20] K. Nagel, D.E. Wolf, P. Wagner, P. Simon, Two-lane traffic rules for cellular automata: A systematic approach, Phys. Rev. E 58 (2) (1998) 1425.
[21] J.A. Cuesta, F.C. Martínez, J.M. Molera, A. Sánchez, Phase transitions in two-dimensional traffic-flow models, Phys. Rev. E 48 (6) (1993) R4175.
[22] E. Brockfeld, R. Barlovic, A. Schadschneider, M. Schreckenberg, Optimizing traffic lights in a cellular automaton model for city traffic, Phys. Rev. E 64 (5) (2001) 056132.
[23] X. Li, J. Sun, Intersection multi-objective optimization on signal setting and lane assignment, Physica A: Stat. Mech. Appl. 525 (2019) 1233–1246.
[24] H. Zhao, X. Liu, X. Chen, J. Lu, Cellular automata model for traffic flow at intersections in internet of vehicles, Physica A: Stat. Mech. Appl. 494 (2018) 40–51.
[25] C. Jiang, T. Chen, R. Li, L. Li, G. Li, C. Xu, S. Li, Construction of extended ant colony labor division model for traffic signal timing and its application in mixed traffic flow model of single intersection, Concurr. Comput. 32 (7) (2020) e5592.
[26] C. Chen, Q. Xu, M. Cai, J. Wang, B. Xu, X. Wu, J. Wang, K. Li, C. Qi, A graph-based conflict-free cooperation method for intelligent electric vehicles at unsignalized intersections, in: 2021 IEEE International Intelligent Transportation Systems Conference, ITSC, IEEE, 2021, pp. 52–57.
[27] L. Cruz-Piris, M.A. Lopez-Carmona, I. Marsa-Maestre, Automated optimization of intersections using a genetic algorithm, IEEE Access 7 (2019) 15452–15468.
[28] W. Wu, Y. Liu, Y. Xu, Q. Wei, Y. Zhang, Traffic control models based on cellular automata for at-grade intersections in autonomous vehicle environment, J. Sensors 2017 (2017).
[29] R. Jiang, Q. Wu, Cellular automata models for synchronized traffic flow, J. Phys. A: Math. Gen. 36 (2) (2002) 381.
[30] K.C. Dey, A. Rayamajhi, M. Chowdhury, P. Bhavsar, J. Martin, Vehicle-to-vehicle (V2V) and vehicle-to-infrastructure (V2I) communication in a heterogeneous wireless network–performance evaluation, Transp. Res. C 68 (2016) 168–184.
[31] Y. Lu, X. Xu, C. Ding, G. Lu, A speed control method at successive signalized intersections under connected vehicles environment, IEEE Intell. Transp. Syst. Mag. 11 (3) (2019) 117–128.
[32] T. Wen, P. Lai, et al., Understanding the topological characteristics and flow complexity of urban traffic congestion, Physica A: Stat. Mech. Appl. 473 (2017) 166–177.
[33] X. Chen, B. Xu, X. Qin, Y. Bian, M. Hu, N. Sun, Non-signalized intersection network management with connected and automated vehicles, IEEE Access 8 (2020) 122065–122077.
[34] F.L. Hall, Traffic stream characteristics, Traff. Flow Theory. US Federal Highw. Admin. 36 (1996).
[35] G. Wong, S. Wong, A multi-class traffic flow model–an extension of LWR model with heterogeneous drivers, Transp. Res. Part A: Policy Pract. 36 (9) (2002) 827–841.
[36] Z. Du, B. HomChaudhuri, P. Pisu, Hierarchical distributed coordination strategy of connected and automated vehicles at multiple intersections, J. Intell. Transp. Syst. 22 (2) (2018) 144–158.